Efficient 1018nm high power fiber laser using intracavity tilted FBG ASE filters

Bertrand Morasse*, Alexandre Perron, Dominic Faucher, Pierre-Michel Belzile, Mathieu Vollant Deschênes, Frédéric Faucher, Guillaume Brochu, François Trépanier, Pascal Deladurantaye

ABSTRACT

We present an efficient way to remove unwanted amplified stimulated emission (ASE) in high-power fiber lasers and amplifiers using intracavity chirped tilted fiber Bragg grating (CTFBG) filters. The grating is written with tilted fringes so that the unwanted ASE is reflected into the fiber cladding where it is no longer amplified. Depending on the desired emission wavelength and active fiber, one or several filters are spliced within the active fiber to suppress ASE before it reaches a detrimental power. Numerical simulations clearly show that adding the filters allows amplification in configurations that would just be impossible due to the onset of ASE. The filter bandwidth and extinction, and the maximum allowed active fiber length between each filter are also computed depending on the core/cladding diameter ratio of the active fiber used and the targeted emission wavelength. As an example, a fiber laser at 1018 nm is assembled in a 20/400µm core/cladding diameter ytterbium fiber that is cladding pumped at 976 nm. Two CTFBGs with 20 dB attenuation from 1025 nm to 1070 nm are spliced within the 6-meter-long ytterbium fiber. 432 W of laser emission at 1018 nm is efficiently achieved at 77% slope efficiency with respect to the absorbed pump power. The extinction between the 1018 nm signal and the ASE is greater than 50 dB. Removing the ASE filters from the cavity clearly leads to only self-pulsation of the ASE between 1030 nm and 1050 nm, no generation of 1018 nm light was possible. The measured thermal slope of the filters shows scalability above the kW level. Demonstration at 1908 nm with a 25/400 core/cladding diameter thulium doped fiber is also done. Tests were done to inscribe the CTFBG directly in an ytterbium fiber for simpler implementation and avoid additional splicing.

Keywords: ASE filter, chirped tilted fiber Bragg grating, high power fiber laser and amplifier, short or long wavelength emission

1. INTRODUCTION

ASE is detrimental in many fiber laser and amplifier designs, especially when trying to obtain high gain[1], high energy[2], or emission at shorter or longer wavelengths than the doped active ion naturally emits in its host material[3]. Several methods have been proposed to remove unwanted ASE in the past. Large core/cladding ratio with small fiber length can favor the gain at shorter wavelength[4], but the larger core degrades the beam quality and the smaller cladding limits the possible injected pump power. Optical fiber with a W-type refractive index profile can suppress ASE at longer wavelengths, but they are typically limited to small core diameters[5]. Photonics bandgap fiber could also be used to suppress ASE[6], but this implies manufacturing a challenging inner fiber structure with very precise tolerancing. Using an isolator within an amplifier was also proposed[7], but this only removes counter-propagating ASE and would not work in a bidirectional fiber laser cavity. Adding a bandpass filter directly into the cavity was also investigated[8], but its free space approach typically introduces high losses into the cavity and cannot handle a large amount of power.

CTFBGs have been proven in the past to be very effective to suppress stimulated Raman scattering in multi-kilowatt fiber laser[9]. In this paper, we present the use of such gratings to remove ASE in high power integrated monolithic fiber lasers and amplifiers. CTFBG can be inscribed in mostly all optical fibers with a precise control of its extinction band and with low insertion loss. Compared to the previous described methods, low insertion loss and multi-kilowatt power handling can be achieved. This approach also allows using smaller core/cladding diameter ratios, which gives better beam quality and allows higher pump power. Many fiber laser or amplifier configurations can benefit from this component. In this paper, we demonstrate a short wavelength emission at 1018 nm in a 20/400µm core/cladding diameter ytterbium fiber. We show with simulations that CTFBG can be implemented along the active fiber length to suppress unwanted ASE before it gets significantly amplified. The simulator predicts the required extinction and bandwidth of the filters and the maximum possible active fiber length between each filter. We also simulate the case of a

*bmorasse@teraxion.com; phone 1 418 658-9500; www.teraxion.com

Proceedings SPIE, Photonics West, LASE, Fiber Lasers XXI: Technology and Systems, paper 12685-13 (2024)

1726 nm thulium fiber laser that can be directly pumped at 790 nm due to the ASE filters, which includes a cladding pump reflector at the end of the cavity to further increase the output power. We could also predict that the filtered ASE that is deviated into the cladding does not get amplified for typical double cladding amplifier or laser designs. We verify the simulations by operating a fiber laser at 1018 nm with a 20/400µm fiber and another one at 1908 nm with a 25/400µm thulium fiber. We clearly confirm that signal amplification was only possible when using these filters. We also validate that the CTFBG can be directly inscribed into the active fiber to avoid additional splicing in the system with still considerable achievable output power.

2. TYPICAL CONFIGURATION WITH ASE FILTERS

A typical configuration of a linear fiber laser cavity with ASE filters is shown in Figure 1. The CTFBG are written with tilted fringes[9] so that the unwanted ASE is reflected into the fiber cladding where it is no longer amplified. To maximize the signal conversion efficiency, the ASE filters must be inserted within the active fiber length to attenuate the ASE before it gets significantly amplified. If the filter were placed at the output of the fiber laser, the output ASE would also be reduced, but its downstream amplification in the active fiber would prevent the desired signal power to get its full amplification in many chosen configurations.

The CTFBGs are inscribed in standard passive germanium-doped optical fiber that is compatible with the ytterbium fiber as typically done for the high reflectivity grating (HR) and output coupler (OC). The ASE filters are then spliced within the Yb fiber. They are recoated with low index polymer to allow transmission of the pump light.

The other components of the cavity are standard. The desired amount of pump power from the diodes is injected into the cladding of the fiber laser cavity using a fiber pump combiner (FPC). A second pump combiner, not shown in Figure 1, could be added in counter-propagation if bi-direction pumping is desired. A cladding mode stripper (CMS) is added to remove all residual cladding pump light and an end cap (EC) with anti-reflective coating is spliced at the output of the cavity to avoid end facet damage.

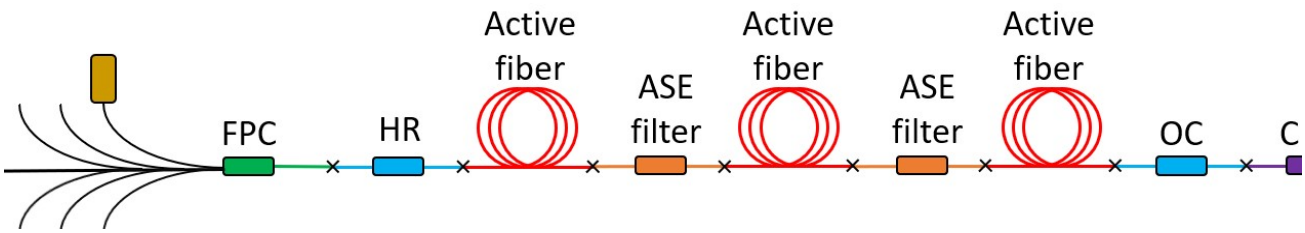

Figure 1. A typical configuration of a fiber laser with ASE filters.

3. SIMULATIONS

3.1 Simulation of the ASE filtering

A standard two-level rate equation model allows us to precisely model the behavior of fiber lasers systems[10,11]. Typical transition cross-sections for ytterbium and thulium ions in silica were used as found in literature[11,12] or given by manufacturers for the fibers used in our experiments.

As shown in Figure 2(a), amplifying a 40 W signal at 1018 nm with 6 meters of 20/400 ytterbium fiber using 400 W of pump power at 976 nm leads to rapid absorption of the signal with the onset of a strong ASE power in both directions. The generated forward and backward ASE power are mainly distributed between 1030 nm and 1090 nm as shown in Figure 3(a).

In the model, we can add discrete wavelength dependent losses at specific positions along the active fiber length to simulate the attenuation effect of the CTFBGs. Figure 2(b) shows the simulation of the same 6-meter ytterbium fiber amplifier, but with the addition of a CTFBG every 2 meters of active fiber as depicted in Figure 1. The positions of the ASE filters are indicated with dotted lines in the graph of Figure 2(b). In the simulation, we fixed the filters' extinction at 20 dB from 1020 nm to 1085 nm. A 0.25 dB signal loss at each filter is considered, which includes the typical loss of the filter and splice losses altogether. We can readily see in Figure 2(b) that the filters adequately remove the ASE in both

directions allowing efficient amplification of the 1018 nm signal. The output ASE spectrum in both directions is very strong without ASE filters as shown in Figure 3(a). When adding the two ASE filters, the peak ASE power decreases by a factor greater of 50 dB as displayed in Figure 3(b); we can see that the ASE is well attenuated within the 1020 nm to 1085 nm bandwidth of the ASE illustrated with the two dotted lines.

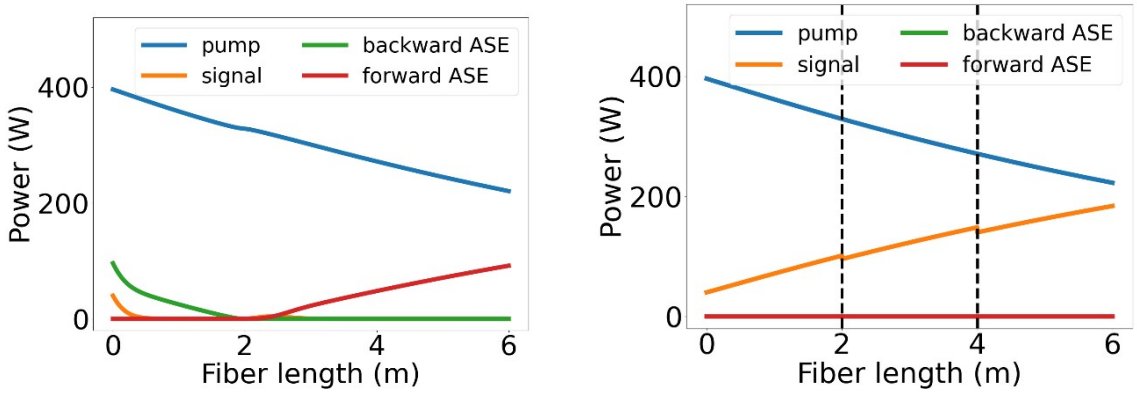

(a) without ASE filter (b) with two ASE filters located at the dotted lines

Figure 2. Simulations of a 20/400 ytterbium 1018 nm amplifier cladding pumped at 976 nm.

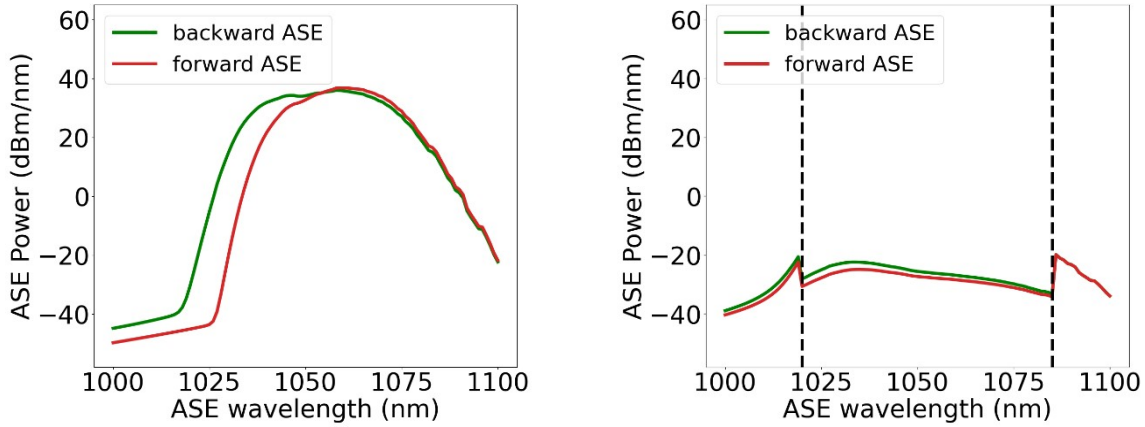

(a) without ASE filter (b) with two ASE filters inserted in the cavity

Figure 3. Simulated output ASE spectra of a 20/400 ytterbium 1018 nm amplifier cladding pumped at 976 nm.

3.2 Optimization of the ASE filter parameters

The simulation model is very useful to optimize the ASE filter parameters. Figure 4(a) shows the copropagating output ASE spectrum of a 1018 nm 20/400 ytterbium amplifier. The difference is that we used two ASE filters with a narrower bandwidth. In this case, the rejection bandwidth of ASE filter, indicated by the vertical dotted red line, is ranging from 1020 nm to 1060 nm. ASE is clearly emitted above 1060 nm, outside of the filter's extinction band. A wider ASE filter bandwidth is therefore required for efficient ASE suppression. We can also see that significant ASE is still generated within the filter bandwidth at 1040 nm, meaning that a filter extinction is too low or adding a third ASE filter would be required.

Figure 4(b) shows the relative maximum output signal power of a 20/400 ytterbium amplifier at 1030 nm as a function of the ASE filter extinction located in the middle of the 12-meter length active fiber. We can readily see that a 20 dB

extinction allows a very efficient amplification of the signal, while an extinction higher than 30 dB does not bring any further output signal improvement. Compared to the simulation at 1018 nm the previous sections, a much longer active fiber length can be used at 1030 nm before inserting an ASE filter. Typical cross-sections of ytterbium doped silica fibers[11] favor signal gain at 1030 nm compared to 1018 nm, which therefore reduces the ASE generation.

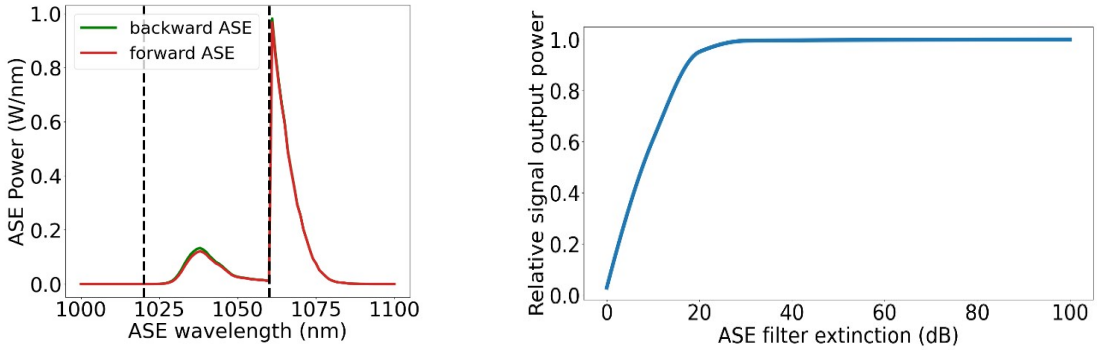

(a) (b)

Figure 4. (a) ASE output spectrum when using an ASE filter with a too narrow stopband bandwidth shown with the dotted lines and (b) relative output power as a function of the ASE filter extinction.

There is a tradeoff between the filter extinction, the number of filters inserted into the active fiber, and the distance between each filter for a given configuration. For instance, a simulation was done to amplify a 1726 nm 10W signal into a double cladding 25/250 thulium amplifier co-pumped with 250 W of power at 790 nm. Amplifying such a short wavelength signal in this double-cladding thulium configuration leads rapidly to strong ASE generation from 1800 nm to 1950 nm. No signal amplification at all can be achieved when the thulium fiber length is greater than 0.2 m, so adding ASE suppression filters is required to get efficient amplification using longer active fiber. Figure 5 shows the maximum total allowed thulium fiber length as a function of the filter's extinction and the number of filters spliced within the cavity. A total filter insertion loss of 0.25 dB per filter was considered, which includes the two splice losses per filter. The maximum fiber length is determined when the output signal saturates, which means that no significant increase in the output signal (<1%) is obtained when adding further active fiber length. The higher the number of filters and the higher their extinction, the longer the total thulium length we can use, which allows more pump absorption and thus higher output signal. A graph of the longitudinal evolution of the power using seven 30 dB filters ASE filters is shown in Figure 6(a).

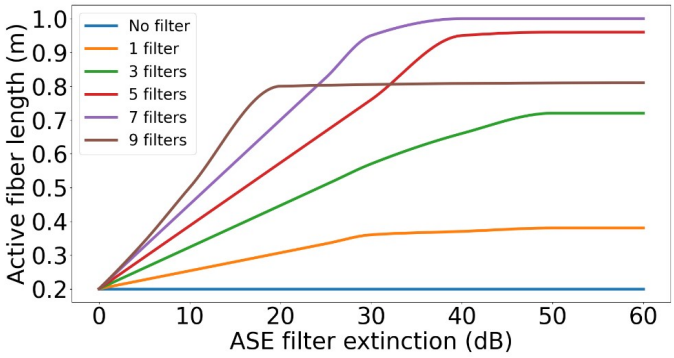

Figure 5. The maximum total active fiber length before the output signal saturates as a function of the filter extinction and the quantity of filters spliced into active fiber for a 1726 nm double cladding Tm amplifier pumped at 790 nm.

However, the active fiber length never exceeds 1.0 m in the example shown in Figure 5. Adding more filters or increasing their attenuation does not allow longer active length, or in other words, higher output signal. The reason is that already half the pump power is absorbed after this length, which does give enough inversion of the thulium ions to

get gain at shorter wavelengths[13]. The system is therefore not limited by the ASE anymore, but fundamentally by the cross-sections of the active ions. Adding too many filters can even decrease the output power due to the added insertion and splice losses of each filter. In the example of Figure 5, using 7 filters would maximize the output signal power. Using 9 filters decreases the achievable active fiber length and thus output signal power.

Counter-pumping could be used to further increase the thulium inversion and thus the output signal power. But since the residual co-pumping power is significant, a pump reflector[14] could be added at the end of the amplifier to recycle the unused pump power. Such component is made of a high reflectivity grating photoinscribed in the silica fiber cladding to reflect the residual pump power back into the active fiber[14]. Figure 6(b) demonstrates the gain in the output signal when adding a 100% pump reflector at the end of the amplifier compared to the reference amplifier simulated in Figure 6(a). The residual unused pump power is cut in half and the output signal goes from 48 W to 70 W when adding the pump reflector. Combining ASE filters and a pump reflector is therefore interesting for short signal wavelength emission in double cladding laser or amplifier due to the high level of inversion required.

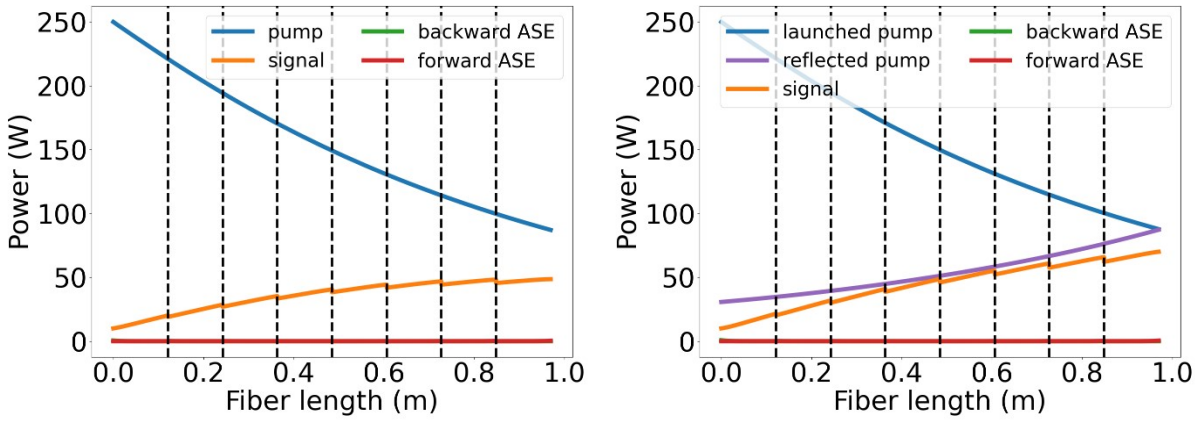

Figure 6. (a) simulation of a 1726 nm thulium amplifier cladding pumped at 790 nm operated with 7 ASE filters indicated by the vertical dotted lines and (b) the same amplifier but with a 100% pump reflector located at the end of the amplifier.

3.3 Cladding modes overlap with the dopant

The CTFBG couples the core power mainly into the cladding of the fiber. In most high-power fiber lasers, since the cladding is surrounded by a low refractive index polymer, the filtered ASE can thus be guided along the cladding. We simulated if this cladding ASE could be amplified by the active fiber. The simulation was done using 6 meters of 20/400 µm core/cladding diameter ytterbium doped fiber. An input core power of 5 W at 1040 nm is injected, which is a typical wavelength for the ASE generation in this configuration, and 100 W of cladding pump power at 976 nm. The ytterbium concentration was fixed at 7e26 ions/m^3 to get 1 dB/m of absorption at 976 nm with the cross-sections used. We first start the simulation with a 17 µm mode field diameter for the input power, which is typical for this core numerical aperture (NA) of 0.065. Our model did not allow calculating and injecting cladding modes, but we simply repeated the simulation by changing the ratio of the mode field diameter over the doped diameter region at each run. This approximates the trend of exciting cladding modes with large mode field diameter, which have a small overlap with the doped region. As seen in Figure 7, the amplification becomes gradually less efficient when the ratio of the mode field diameter to the dopant diameter goes below 0.5. This behavior is expected because the overlap of the power with the ytterbium inverted ions in the core is too small to get an efficient energy transfer. Knowing that cladding modes have typically low overlap with the doped core in a double cladding fiber[15], we can expect that the ASE reflected in the cladding will not be amplified. Cladding amplification is still less likely to happen considering that the high power injected core signal power is strongly overlapping with the dopant and will take most of the gain[16]. More complete simulations including core and cladding modes would be required to get a better understanding, but we confirm in the experiments presented in the next section that no cladding light amplification was measured.

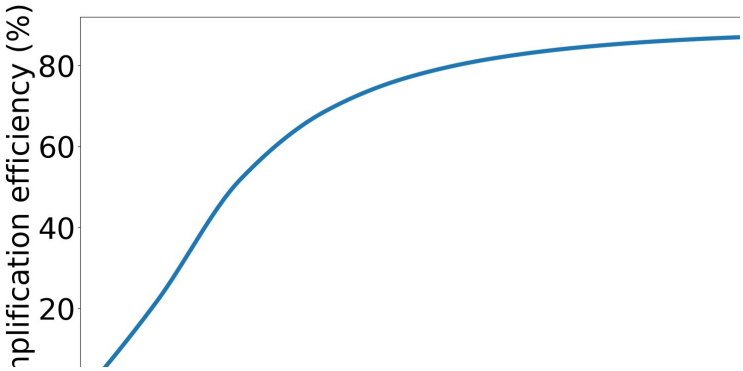

Figure 7. Simulation of the amplification efficiency of ASE coupled in the cladding as a function of the mode overlap with the active dopant in a 20/400 double cladding ytterbium amplifier.

4. EXPERIMENTS

4.1 Fiber laser at 1018 nm

To test the efficiency of ASE filters, we assembled a fiber laser cavity emitting at 1018 nm using a 20/400 core/cladding diameter ytterbium fiber with 0.065/0.46 core/cladding numerical aperture (NA). CTFBGs were photoinscribed in a matched 20/400 µm passive germanium doped fiber with the same core NA. The measured attenuation curve of the CTFBG is shown in Figure 9. Two ASE filters were inserted in the 6-meter-long ytterbium fiber as detailed in Figure 8. The ytterbium fiber was therefore cut into 3 pieces of 2 meters in length. The 99.5% high reflectivity grating (HR) and 10% output coupler (OC) were inscribed for 1018 nm in the same matched passive fiber. Two pump diodes of 400 W at 976 nm without wavelength stabilization were injected into the active fiber with a standard 6+1→1 fiber pump combiner (FPC) with 200µm/0.22NA pump port and 400µm/0.46NA output. The 20/400 ytterbium active fiber had a measured cladding absorption around 1.1 dB/m when the pump central wavelength was tuned at 976 nm. A cladding mode stripper (CMS) was added to remove all residual cladding pump light. An end cap (EC) with anti-reflective coating was spliced at the output of the cavity to avoid end facet damage.

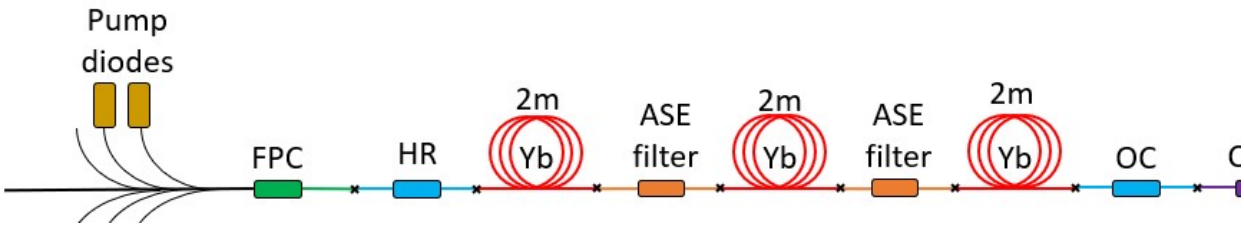

Figure 8. Configuration of the 20/400 Yb fiber laser at 1018 nm with two ASE filters.

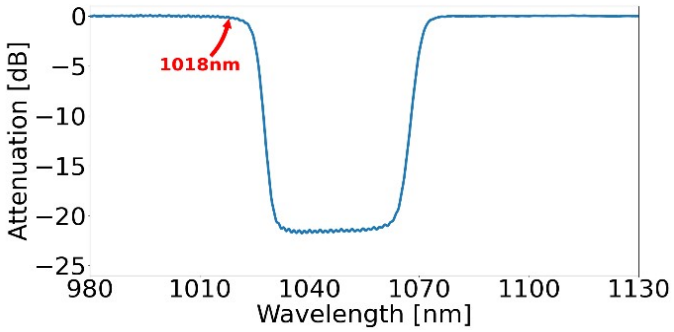

Figure 9. Attenuation spectrum of the ASE filters used in the simulation and experiments.

As shown in Figure 10(b), it was only possible to generate light at 1018 nm when using the CTFBG ASE filters; otherwise, only self-pulsing of the ASE between 1030 nm to 1050 nm was measured when removing the ASE filters. An output signal of 432 W was obtained with a slope efficiency of 77% with respect to the absorbed pump power at 976 nm as shown in Figure 10(a). At the maximum output power of the laser, less than 1 mW of ASE power was measured in the four unused pump ports of the pump combiner; this confirms that no amplification of ASE power occurs in the cladding as predicted by the simulations. The cladding modes excited by the CTFBG have therefore a low overlap with the doped region.

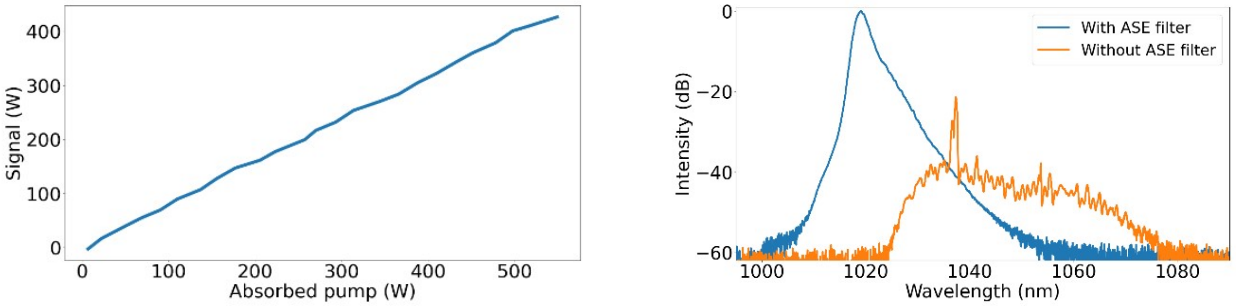

(a) (b)

Figure 10. (a) Slope efficiency with respect to the absorbed pump power and (b) the output spectrum of the 1018 nm fiber laser with and without the ASE filters.

The signal thermal slope of the filters was measured at 1µm with free convection without any cooling. This measurement was done by launching core signal at a wavelength outside the attenuation band of the ASE filter. The associate temperature rise with respect to the signal power was measured with a high-resolution thermal camera. We obtained a value below 0.10°C/W as shown in Figure 11. This easily allows operation above 1 kW without coating thermal damage when properly heatsinked with conduction onto a metal plate or in a groove. The measured insertion losses of the grating were below 0.1 dB at the signal wavelength. The output power was limited by self-pulsing of the ASE around 1040 nm. A higher extinction of the CTFBGs or shorter ytterbium lengths in between each would be required to reach higher power.

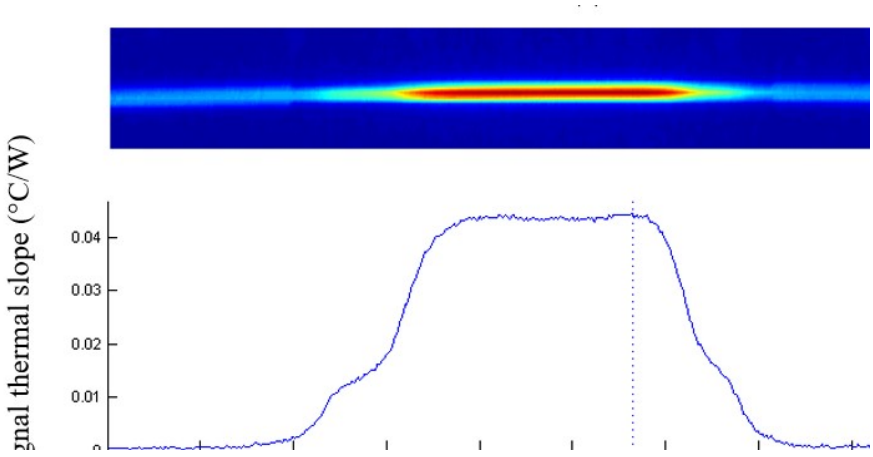

Figure 11. Typical thermal image and thermal slope of an ASE filter in free convection when launching 1µm wavelength core signal power at a wavelength outside the attenuation band of the filter.

4.2 Fiber laser at 1908 nm

The ASE filter concept was also tested with a thulium fiber laser linear cavity as depicted in Figure 12. We used 4 meters of thulium doped double cladding fiber with a core/cladding ratio of 25/400 µm and a measured cladding pump absorption of 2 dB/m at 790 nm. The core/cladding numerical aperture was 0.09/0.46. The HR and OC reflectivity at 1908 nm were 99.5% and 10% respectively. 50W of pump power at 790 nm was launched in co-propagation using a standard 6+1→1 pump combiner with 200µm/0.22NA fiber pump ports. The ASE filter and HR/OC reflectors were inscribed in a passive germanium doped with the same core/cladding parameters than the active fiber.

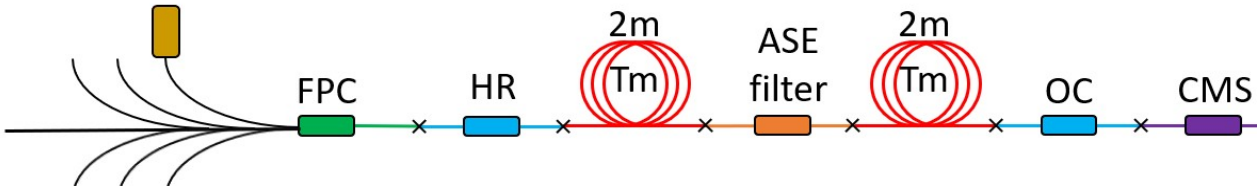

Figure 12. Configuration of the 25/400 thulium fiber laser at 1908 nm with one ASE filter.

The measured attenuation spectrum of the ASE filter used for the 1908 nm fiber laser is shown in Figure 13(a). The 10 dB attenuation bandwidth ranges approximately from 1935 nm to 1990 nm. As illustrated in Figure 13(b), only self-pulsing of the ASE between 1970 nm to 1980 nm is measured without the CTFBG. When adding the ASE filter in the middle of the cavity, amplification at 1908 nm occurs with an ASE rejection higher than 50 dB. Decreasing the cladding diameter to 250 µm would also favor 1908 nm amplification, but using a large 400µm cladding diameter in this design increases the amount of launchable pump power. For a given core diameter, the thermal load of the active fiber is also greatly decreased with a large cladding. Thulium doped fibers require high doping levels to maintain a good conversion efficiency with 790 nm cladding pumping[17], so increasing the cladding diameter is an effective way to decrease the pump absorption.

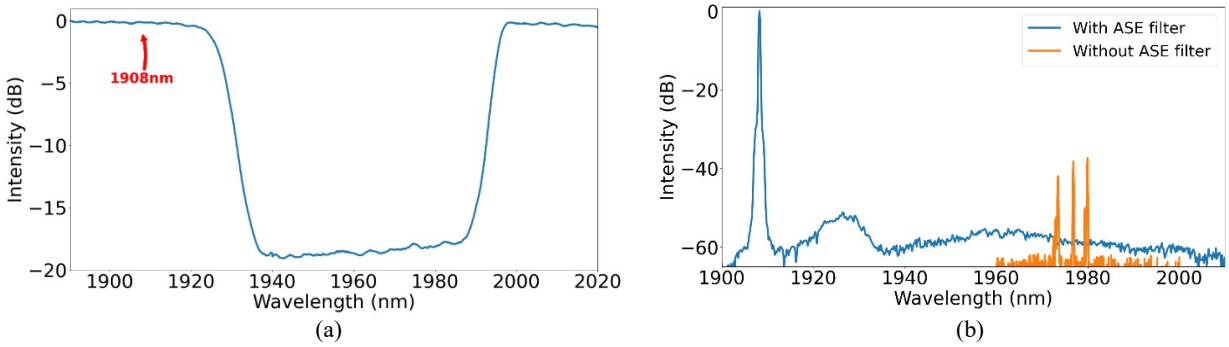

Figure 13. (a) Attenuation spectrum of the ASE filter used and (b) output spectrum of the thulium fiber laser at 1908 nm with and without the ASE filter.

4.3 ASE filter inscribed directly into the active fiber

The above experiments at 1018 nm and 1908 nm have been done by inscribing the ASE filters in passive germanium doped fibers and splicing them within the ytterbium or thulium doped active fibers. In order to avoid the splicing process and the associated splice losses, we tested the inscription of the CTFBG directly into the active fiber using a femtosecond laser. An example of the attenuation spectrum of a CTFBG ASE filter written into a 20/400 ytterbium fiber is shown in Figure 14. The measured signal thermal slope at 1018 nm with free convection in the air was 1.8°C/W, which is much higher than the 0.12°C/W measured in the passive fiber for the 1018 nm experiment. Such high signal thermal slope for FBG inscribed directly into an ytterbium fiber has also been reported previously[18]. The filter was then fixed onto a metal plate to heatsink it and the signal thermal slope dropped to 0.14°C/W. With this lower thermal slope, a maximum transmitted signal power of 350 W is predicted before reaching the maximum coating recommended operation temperature of 85°C. The measured signal insertion loss at 1018 nm was as low as 0.03 dB.

	Insertion losses (dB)	Signal thermal slope under free air convection (°C/W)	Maximum predicted output power when heatsinked (W)
Passive Ge fiber	< 0.1	<0.10	> 1000
Active Yb fiber	< 0.1	1.8	350

Table 1. Comparison of the insertion losses, signal thermal slope under free air convection and maximum predicted output power when properly heatsinked of typical ASE filters inscribed in passive germanium doped fiber or active ytterbium doped fiber.

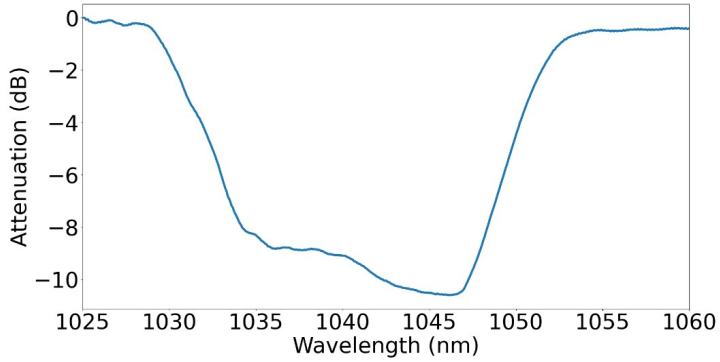

Figure 14. Attenuation profile of an ASE filter written directly into an ytterbium doped fiber.

A CTFBG could also be written directly through the coating of the active fiber to avoid the strip and recoat process potentially giving a higher mechanical strength[19] and allowing a higher pump power transmission[9]. This also offers the possibility to easily write as many ASE filters as required into the same piece of doped fiber.

5. CONCLUSION

We demonstrated that adding chirped tilted fiber Bragg gratings within an active fiber length was an efficient and simple way to suppress ASE. This allows the amplification of light at uncommon wavelengths in high power fiber lasers and amplifiers. This component can be written directly into the active fiber, or into a matched passive fiber spliced in between active fiber segments. Using a typical fiber amplifier simulation model, we could optimize the extinction, bandwidth and number of ASE filters needed for a given design. A 1018 nm ytterbium and a 1908 nm thulium doped fiber lasers were realized to demonstrate the concept of ASE filtering. Direct writing of an ASE filter into an ytterbium fiber was also realized.

REFERENCES

[1] Laming, R. I., Zervas, M. N. and Payne, D. N., "Erbium-doped fiber amplifier with 54 dB gain and 3.1 dB noise figure," IEEE Photonics Technology Letters 4(12), 1345-1347(1992).

[2] Renaud, C. C., Offerhaus, H. L., Alvarez-Chavez, J. A., Nilsson, J., Clarkson, W. A., Turner, P. W., Richardson D. J. and Grudinin, A. B., "Characteristics of Q-switched cladding-pumped ytterbium-doped fiber lasers with different high-energy fiber designs," IEEE Journal of Quantum Electronics 37(2), 199-206 (2001).

[3] Desurvire, E., "Erbium-doped fiber amplifiers, 2 volume set" Wiley, 2nd edition (2002).

[4] Yan, P., Wang, X., Wan, Z., Huang, Y., Li, D., Xiao, Q. and Gong, M., "A 1150-W 1018-nm fiber laser bidirectional pumped by wavelength-stabilized laser diodes," IEEE Journal of Selected Topics in Quantum Electronics 24(3), 0902506 (2018).

[5] Chen, S., Chen, Y., Liu, K., Sidharthan, R., Li, H., Chang, C. J., Wang, Q. J., Tang, D. and Yoo, S., "All-fiber short-wavelength tunable mode-locked fiber laser using normal dispersion thulium-doped fiber," Optics Express 28(12) 17570-17580 (2020).

[6] Kong, F., Gu, G., Hawkins, T. W., Jones, M., Parsons, J., Kalichevsky-Dong, M. T., Palese, S. P., Cheung, E. and Dong, L., "Efficient 240W single-mode 1018nm laser from an ytterbium-doped 50/400μm all-solid photonic bandgap fiber," Optics Express 26(3), 3138-3144(2018).

[7] Zervas, M. N., Laming, R. I. and Payne, D. N., "Efficient erbium-doped fiber amplifier with an integral isolator," Proceedings of Optical Amplifier and Their Applications, FB2(1992).

[8] Simeonidou, D., Yu, A., O'Mahony, M. J., Yao, J. and Siddiqui A.S., "Erbium-doped fiber pre-amplifier with an integral band-pass filter," Proceedings of IEE Colloquium on Optical Detectors and Receivers (1993).

[9] Brochu, G., Gouin, S., Brown-Dussault, E. Huneault, M., Faucher D. and Trépanier, F., « High performance FBG-based components for kilowatt fiber lasers power scaling," Proceedings of SPIE 11261, 112610P (2020).

[10] Morasse, B., Hovington, C., Chatigny, S. and Piché, M., "Accurate modeling and experimental validation of a singlemode 4 W output power double cladding erbium ytterbium fiber amplifier," Proceedings of Photonics North 6453(2006).

[11] Paschotta, R., Nilsson, J., Tropper, A. C. and Hanna, D. C., "Ytterbium-doped fiber amplifiers," IEEE Journal of Quantum Electronics, 33(7), 1049-1056(1997).

[12] Agger, S. D. and Povlsen, J. H., "Emission and absorption cross section of thulium doped silica fibers," Optics Express 14(1), 50-57(2005).

[13] Chen, S., Jung, Y., Alam S.-U., Richardson D. J., Sidharthan, R., Ho, D., Yoo S. and Danier J. M. O., "Ultra-short wavelength operation of thulium-doped fiber amplifiers and lasers," Optics Express 27(25), 36699-36707(2019).

[14] Pelletier-Ouellet, S., Talbot, L., Mailloux, A., Trépanier, F. and Bernier M., "Femtosecond inscription of large-area fiber Bragg gratings for high-power cladding pump reflection," Optics Letters 47(19), 4989-4992(2022).

[15] Zervas, M. N and Kim, J., "Effective absorption in cladding-pumped fibers," Proceedingsof SPIE 7914, 79141T-1 (2011).

[16] Gong, M., Yuan, Y., Li, C., Yan, P., Zhang, H. and Liao, S., "Numerical modeling of transverse mode competition in strongly pumped multimode fiber lasers and amplifiers," Optics Express 15(6), 3236-3246(2007).

[17] Jackson, S. and Mossman, S., "Efficiency Dependence on the Tm3+ and Al3+ Concentrations for Tm3+-Doped Silica Double-Clad Fiber Lasers," Applied Optics 42(15), 2702-2707(2003).

[18] Bernier, M., Vallée, R., Morasse, B., Desrosiers, C., Saliminia, A. and Sheng, Y., "Ytterbium fiber laser based on first-order fiber Bragg gratings written with 400nm femtosecond pulses and a phase-mask," Optics Express 17(21), 18887-18893(2009).

[19] Bernier, M., Trépanier, F., Carrier, J. and Vallée, R., "High mechanical strength fiber Bragg gratings made with infrared femtosecond pulses and a phase mask." Optics Letters 39(12), 3646-3649(2014).